Investigation of roll bite behavior with various cold rolling conditions using semi-analytic solutions of von karman's rolling equation

R.-M. Guo

This article proposes a semi-analytical solution of von Karman's rolling equation on the elastic foundation. The roll indentation is considered as the spring compression of the elastic foundation of the work roll. A non-circular contact arc is obtained naturally as a part of the solution of the governing equation. Two elastic zones and four plastic zones are included. Hooke's law is applied in elastic zones, von Mises' yield criterion is used in plastic yielding and unyielding zones, and material stress-strain curves are employed in plastic loading and unloading zones. The solution of each zone was derived separately and a computer program was designed accordingly. The computing time is very short and the required core memory is very small. The results show that the compressive stress curves form a "friction hill" while the shape of the normal stress curve depends on the rolling parameters. A typical cold rolling case is selected as the basic study case. The results of this proposed model and the popular Bland-and-Ford model are shown to make comparison between these two models. Key rolling parameters included in the comparison results are the entry gage, the exit gage, the entry tension, the exit tension, the work roll diameter, the yield stress, and the friction coefficient. Rolling feasibility derived from this proposed model is not only on the existence of the convergent solution but also on whether or not the solution can follow the properties of the rolled material.

Keywords: Slip friction - Stress-strain curve - Rolling model - Rrolling mill - Separation force - Von Karman - Von Mises - Yield criterion

INTRODUCTION

The rolling equation was derived first by von Karman in 1925 [1]. It is a simple equilibrium equation of an infinitesimal element in the roll bite. The equation includes three unknowns – the normal stress *s*, the compressive stress σ, and the thickness distribution *h*. Two additional equations are required for the unique solution. Most conventional studies assume a circular contact arc calculated from an equivalent roll diameter and von Mises' yield criterion dominated in the roll bite [2,3,4]. The governing equation, the contact arc, and the yield criterion were further simplified so as to obtain closed form and/or solvable solutions. As a result, a specific solution can be applied only to a specific rolling condition which agrees with the imposed assumptions. For instance, Sims'[2], Bland-and-Ford's [3], and Robert's [4] equations have been applied broadly in hot mills, cold mills, and temper mills respectively. Later, Fleck and Johnson proposed a so-called "double dip" contact arc to solve the foil mill problem [5]. Continuous efforts by them and their followers have improved the performance of this new non-circular arc model [6,7]. However, the application range has been limited in the ultra-thin gage rolling area. Most prior investigations apply von Karman's equation and von Mises' yield criterion, but the material stress-strain curve is not taken into account. And the normal and tensile stresses are not bounded to the yield and ultimate stresses of the material. The contact arc is either assumed to be a circular arc or assigned by a specific function.

This article proposes a simple model which is von Karman's equation on the elastic foundation. The work roll is treated as the elastic foundation. The differential form of Hertzian cylindrical flattening equation [8] is employed to calculate the spring constant of the elastic foundation. Since the roll indentation has been considered in the governing equation, this model does not apply the equivalent roll diameter widely used in the conventional models. The roll bite is divided into six zones from the entry side to the exit side including the elastic deformation zone, the plastic yielding zone, the plastic loading stress-strain zone, the plastic unloading stress-strain zone, the plastic unyield-

Remn-Min Guo

Tenova I2S
475 Main St, Yalesville, Connecticut 06492

Paper presented at the Int. Conf. ROLLING 2013, Venice 10-12 June 2013, organized by AIM

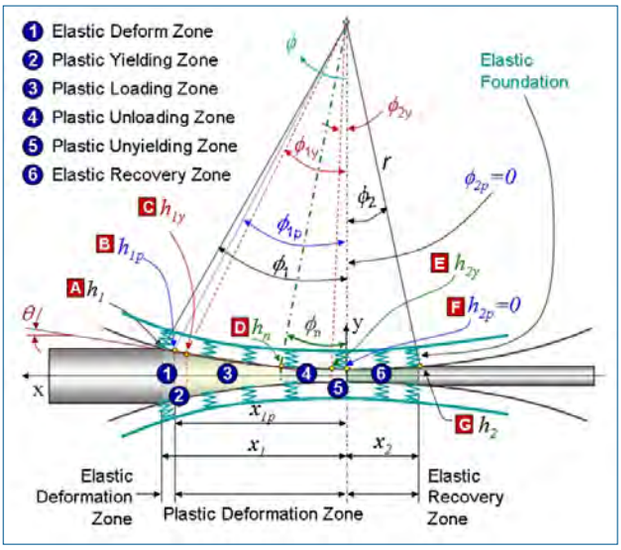

Fig.1 - Von Karman Equation on Elastic Foundation

Fig. 1 - Equazione di von Karman per fondazione elastica

ing zone, and the elastic recovery zone. The elastic zones obey Hooke's law. von Mises' yield criterion is applied in the yielding and unyielding zones. The general exponent equation for the material stress-strain relationship is employed in the loading stress-strain zones while a combined stress-strain curve is used in the unloading stress-strain zone. Boundary conditions are imposed at two ends of the roll bite including the entry/exit thickness, the entry/exit tension, and zero normal and shear stresses at both ends. The join points between two adjacent zones satisfy the characteristics of two zones, and also play important roles to transfer the boundary conditions from two ends toward the core portion of the roll bite. Two elastic zones always present, however, four plastic zones may not appear simultaneously depending on the rolling conditions. This method is very straight-forward with no specific assumptions and no specified contact contours. The average computing time of 28ms from 23 test cases is nearly nothing when compared with that from other models due to less iteration in this model.

VON KARMAN'S EQUATION ON ELASTIC FOUNDATION

The detailed derivation of von Karman's equation and the solution of each zone can be found in the references [9,10]. The followings are a summary of the findings. Figure 1 shows the roll bite geometry and the elastic foundation of the work roll. The variables used in this article are shown in table 1.

Von Karman's Equation on Elastic Foundation

The roll indentation δ can be obtained from the normal stress s divided by a spring constant k, namely, $\delta=2s/k$, where k is the spring constant of the elastic foundation. With the following equations and the assumption of the small roll bite angle,

h:	Thickness (rigid roll)
$\hat{h}$:	Total thickness
s:	Normal stress
r:	Work roll radius
x:	Contact arc distance
E:	Strip Young's modulus
ϕ:	Roll bite angle
θ:	Contact arc angle
σ:	Compressive stress
τ:	Shear stress
μ:	Friction coefficient
η:	-1: entry side, 1: exit side
α:	Strain exponent
k:	Elastic foundation spring constant
Q:	Stress constant
ω:	Modified spring constant
Ψ:	Yield criterion coef., 1/3 for steel
ε:	Engineering strain
σ_c:	Critical tension, $=(1-2\sqrt{\psi-\mu^2})s_y$
Subscript:	
1:	Entry side
2:	Exit side
i:	1 (entry) or 2 (exit)
p:	Plastic zone
y:	Yield point

Tab. 1 - Nomenclature

Tab. 1 - Nomenclatura

$$h = h_1 - r(\phi_1^2 - \phi^2) = h_2 - r(\phi_2^2 - \phi^2), \quad \tau = \mu s, \quad dx = rd\phi$$
$$dh/d\phi = 2r\phi$$
$$\tan\theta = d\hat{h}/2dx = \frac{1}{r}\left(\frac{dh}{d\phi} + \frac{1}{k}\frac{ds}{d\phi}\right) = \frac{1}{r}\left(2r\phi + \frac{ds}{kd\phi}\right), \quad \hat{h} = h + 2s/k$$

One can derive von Karman's equation on the elastic foundation in the following:

$$(1) \quad \left(h + \frac{2s}{k}\right)\frac{d\sigma}{d\phi} = (s-\sigma)\left(2r\phi + \frac{ds}{kd\phi}\right) + 2\eta r\mu s$$

Equation (1) is applicable for any mill type with various rolling conditions. The solution of each characteristic zone will be shown in the following sections.

Solutions of von Karman's Equation on Elastic Foundation

Each characteristic zone possesses a specific solution according to the material properties and the corresponding boundary conditions.

Solutions of Elastic Zones following Hooke's Law

The general normal stress equation for the elastic zone is $s_i=E/h_1(h_i-h)$, where $i=1$ for the entry side and $i=2$ for the exit side. After inserting the above equations into Eq. (1) and integrating both sides, one can get the exact solution for elastic deformation and recovery zones:

$$\sigma\hat{h} = \sigma_i h_i + 2\omega r^2\left(-\frac{(\phi^4-\phi_i^4)}{4} - \eta\mu\frac{(\phi^3-\phi_i^3)}{3} + \phi_i^2\frac{(\phi^2-\phi_i^2)}{2} + \eta\mu\phi_i^2(\phi-\phi_i)\right) + \frac{1}{k}s_\phi^2 \quad (2)$$

The signs of σ_1 and σ_2 are non-positive since only tensile stresses can be applied at both sides of the roll bite. The subscripts of the variables in the roll bite as discussed in this article are used to indicate the bite angle location henceforward. For instance, s_ϕ means the normal stress at the angle ϕ, s_1 means the compressive stress at $\phi=\phi_1$, and so forth.

Solutions of Plastic Yielding and Unyielding Zones Based on the Yield Criterion

At the plastic yielding and unyielding zones, the material deforms due to von Mises' yield criterion and its stress components are smaller than corresponding yield stresses. The normal stress can be obtained from the compressive stress according to von Mises' yield criterion:

$$\frac{ds}{d\phi} = \frac{1}{1+4\mu^2}\left(1-\frac{2\mu^2\sigma}{\sqrt{(1+4\mu^2)\psi s_{yi}^2-\mu^2\sigma^2}}\right)\frac{d\sigma}{d\phi} \quad (3)$$

Inserting the yield criterion and its derivative equation (3) into Eq. (1), after some mathematical steps, one can obtain the following equation:

$$\left\{\left(h+\frac{2s}{k}\right)-\frac{2(s-\sigma)}{k(1+4\mu^2)}\left(1-\frac{2\mu^2\sigma}{\sqrt{(1+4\mu^2)\psi s_{yi}^2-\mu^2\sigma^2}}\right)\right\}\frac{d\sigma}{d\phi} = 2r[(\phi+\eta\mu)s-\phi\sigma] \quad (4)$$

Equation (4) can be solved using the numerical method. The calculation should continue toward the core of the roll bite until arriving at the critical tension σ_c where the material also reaches the entry side yield point. For some rolling cases, the compressive stress will never reach the critical tension, and hence, the entire normal stress distribution is smaller than the yield stress. These cases are similar to the cases of previous investigations without considering the stress-strain curve.

Solutions of Plastic Stress-Strain Zones

The entry side stress-strain equation can be expressed as a simple exponent equation $s=Q\varepsilon^\alpha$. The exit side equation can be obtained similarly so as to satisfy the 0th and 1st order continuity conditions of two adjacent zones. Both equations can be expressed as $s=s(\phi,\varepsilon)$. The governing equation (1) can be applied to obtain the compressive stress σ in these zones:

$$\sigma\hat{h} = \sigma_{y1}\hat{h}_{y1} + \frac{s_\phi^2-s_{y1}^2}{k} - 2r\int_\phi^{\phi_{y1}} s(\phi)(\phi-\mu)d\phi \quad \text{for the entry side}$$
$$\sigma\hat{h} = \sigma_{y2}\hat{h}_{y2} + \frac{s_\phi^2-s_{y2}^2}{k} + 2r\int_{\phi_{y2}}^{\phi} s(\phi)(\phi+\mu)d\phi \quad \text{for the exit side} \quad (5)$$

where the subscripts y_1 and y_2 indicate the entry and exit side yield point respectively. The stress curves from the entry side should proceed first toward the exit side to form complete normal stress s and compressive stress σ curves. The normal stress will increase continuously from the entry side thanks to the increasing strain ε. The compressive stress σ increases also to counterbalance the horizontal force components generated by the increasing normal stress s and shear stress τ. The next step is to calculate the stress components from the exit side toward the entry side so as to find the intercept (the neutral point) with the stress curves calculated from the entry side.

Features of the Proposed Model

The proposed model has four major features differentiated from conventional models. This model applies von Karman's equation on the elastic foundation while the conventional model employs simplified von Karman's equation with some terms neglected. This model considers six characteristic zones – elastic deformation, plastic yielding, plastic loading, plastic unloading, plastic unyielding, and elastic recovery - in the roll bite while the conventional model takes only plastic yielding and unyielding zones into account. This model utilizes the iteration method to obtain the convergent spring constant of the work roll elastic foundation. The conventional model uses the iteration method to have the convergent rolling force with an equivalent work roll diameter. The non-circular contact contour of this model is determined by the governing equation and the roll diameter remains the same. The contact contour of the conventional model remains a circular arc while the roll diameter changes in every iterative step. This model considers the material stress-strain curve and the criterion of rolling feasibility relies on if the solution follows the material properties. The conventional models do not consider the stress-strain curve and the rolling feasibility only depends on the existence of the solution.

CASE STUDIES

Rolling Data and Basic Study Case

The following case studies will focus on a typical cold rolling case with:

Entry Gage	0.024"	Entry Yield	50 ksi	Entry Tension	10 ksi
Exit Gage	0.015"	Exit Yield	50 ksi	Exit Tension	18 ksi
WR Diameter	12"	Strain Exponent 0.125	0.125	Friction Coef	0.04

Young's modulus and Poisson ratio of the strip and the roll are 30,000 ksi and 0.3 respectively. The yield stresses of both sides are assumed to be the same so as to make fair comparison with conventional models. Figure 2 shows the result of this basic case – the blue line represents the normal stress, the pink line does the shear stress, and the yellow line does the compressive stress. All six characteristic zones are marked at the bottom of the chart – ED: Elastic Deformation zone, PY: Plastic Yielding zone, PLS: Plastic Loading Stress-strain zone, PUS: Plastic Unloading Stress-strain zone, PU: Plastic Unyielding zone, and ER: Elastic Recovery zone. Five key nodes shown in diamond shapes are used to indicate the beginning and finishing nodes of characteristic zones. For instance, the 2nd key node is the joint node of characteristic zones of PY and PLS, namely, it is the finishing point of the plastic yielding zone and also the beginning point of the plastic loading stress-strain zone. The 3rd key node is also the neutral point. The top (or bottom) tip of the diamond points to the location of the key node.

The elastic deformation zone is very narrow. von Mises' yield criterion is satisfied at the end of the elastic deformation zone (marked as the 1st key node). The yielding zone decreases the normal stress slightly first and increases later to arrive at the entry yield point (marked as the 2nd key node). The material enters the PLS zone following the given stress-strain curve. As to the exit side, the exit elastic recovery zone is much larger than the elastic deformation zone. As proved in the literature [9], the end point of this zone is always located at x=0 (marked as the 5th key node). At this particular point, von Mises' criterion is satisfied. The material enters the unyielding zone, which brings the normal stress up to the yield point (marked as the 4th key node). After the yield point, the material gets into the PUS zone and the normal stress increases continuously until meeting the normal stress curve from the entry side at the neutral point M (marked as the 3rd key node). At the same time, two compressive stress curves from both sides also meet at the neutral point M. As seen from the chart, the compressive stress curve looks like a conventional "friction hill" with very small gradients on both ends. The normal stress curve looks more like a "platform" with one sharp edge on the entry side and one smoothly descending edge on the exit side. The shear stress is just a fraction of the normal stress due to the small friction coefficient of 0.04. It reverses the sign when crossing the neutral point.

Result Comparison of Two Models

This basic cold rolling case happens to have all six characteristic zones. In fact, two elastic zones always exist while the existences of four plastic zones completely depend on the rolling conditions. Next sections will investigate the influences of various rolling parameters of the entry gage, the exit gage, the entry tension, the exit tension, the roll diameter, the yield stress, and the friction coefficient. Since Bland-and-Ford's model is widely applied in cold rolling process, its normal stress curve is also shown in the figure

Fig. 2 - Stress Components and Characteristic Zones

Fig. 2 - Componenti degli sforzi e zone caratteristiche

for comparison. For convenience, Bland-and-Ford's model will be called BAF and this proposed model will be named KEF henceforward. Since the characteristic zones, the key nodes, and the compressive stress curve are not considered in BAF, whenever those terms are discussed, KEF is the discussion focus in the rest of this article.

BAF is an exact solution of simplified von Karman's equation with a circular contact arc. The shear stress is neglected in von Mises' yield criterion by assuming $1+\mu^2 \sim 1$ in cold rolling process. The term $(s/K-1)d(hK)/d\phi$ is negligible according to Bland and Ford since it is much smaller than $hKd(s/K-1)/d\phi$. $K=1.155s_y$ is the constrained compressive stress. The entire roll bite is dominated by von Mises' yield criterion only. Two elastic zones are not considered in BAF. Two tensile stress boundary conditions are obtained from the yield criterion. An iterative loop is used to obtain the convergent equivalent work roll diameter which is calculated by Hitchcock (or Hertzian) roll flattening equation. On the other hand, KEF is derived from von Karman's equation on the elastic foundation. A complete yield criterion (von Mises or Tresca for different material) is considered. The roll bite is composed of six characteristic zones. The boundary condition of each zone is defined by its previous zone. Two outer elastic zones accept the boundary conditions from the rolling conditions, such as entry and exit gages as well as entry and exit tensions. An iterative loop is needed to ensure the convergence of the spring constant of the elastic foundation of the work roll.

In the following figures, the normal stress and the compressive stress using KEF are shown in pink and yellow respectively. The normal stress curve calculated by BAF is shown in blue. Hertzian roll flattening equation is applied to calculate the spring constant in KEF and the equivalent work roll diameter in BAF. For each particular rolling parameter, there are 21 cases calculated to cover the entire range. The increment is a constant. The results were computed by changing only one particular rolling parameter with other parameters remaining the same as the basic study case. All figures display only the maximum and the minimum cases.

Influences of Entry Thicknesses

Figure 3 demonstrates stress components calculated from KEF and BAF for various entry strip thicknesses. The top chart (Figure 3a) is for the thin gage of 0.018". Two results look very close. The maximal stress of BAF is slightly greater than that of KEF. At the end of elastic zones, the material satisfies the yield criterion. Boundary nodes of BAF are nearly the same as key nodes 1 and 5 of KEF. The normal stress curves of the yielding and unyielding zones from both models are nearly the same. After key nodes 2 and 4, KEF forces the material to follow the stress-strain curve while BAF continues applying the yield criterion. There are trivial differences between two stress curves in the stress-strain zone. It is not easy to find KEF's neutral point from the normal stress because the normal stress curve has the smooth curvature in the neighborhood of the neutral point. But it is very obvious that the intercept point of two compressive stress curves is KEF's neutral point. The compressive stress curve starts from two negative points since the tensile stresses are applied at both ends. As shown in Eq. (1), the compressive stress is used to counterbalance the horizontal force generated by the horizontal components of the normal and the shear stress. For a shallow contact arc like this study case, the small contact angle θ leads to a small horizontal component for the normal stress and a larger horizontal component for the shear stress. The shear stress does not have a strong influential contribution to the horizontal force. Hence, the compressive stress σ grows very slowly from tensile stresses at both sides and turns into compressive stress just before the neutral point. On the other hand, BAF's neutral point can be found easily from the normal stress curve. Two neutral points are very close for this case.

Figure 3b shows the results of the thicker entry gage of 0.036", which makes the bite angle about 3 times bigger. The stress curves are very different as well. Both models show that the neutral point shifts to the exit side. BAF has about the same maximum normal stress while KEF has the maximum normal stress about 10% smaller than the previous case. Since the yield criterion is satisfied at the end of the elastic zones, the starting points of the plastic zone are nearly the same from both models. KEF shows that the normal stress in the entire roll bite is under the yield stress. Only the yielding and the unyielding zones exist, which is the same for BAF. As seen from Figure 3b, the normal stress curves at the exit side are nearly identical, but two curves at the entry side have big differences. The differences may result from the different contact arc (circular arc from BAF and non-circular arc from KEF) and the different governing equation (BAF neglects one term while KEF considers the elastic foundation). KEF shows that the large contact arc leads to the smaller contact angle, the smaller normal stress, and the smaller compressive stress. After the 1st key node, both normal and compressive stresses decreases from the entry side, passes through the minimal point at x=.15" approximately, and increases to meet the stress curves from the exit side at the neutral point (the 3rd key node), which is about 0.05" left to the neutral point predicted by BAF. The compressive stress σ is always negative, which means that the strip elements in the roll bite are subjected to tensile stresses only.

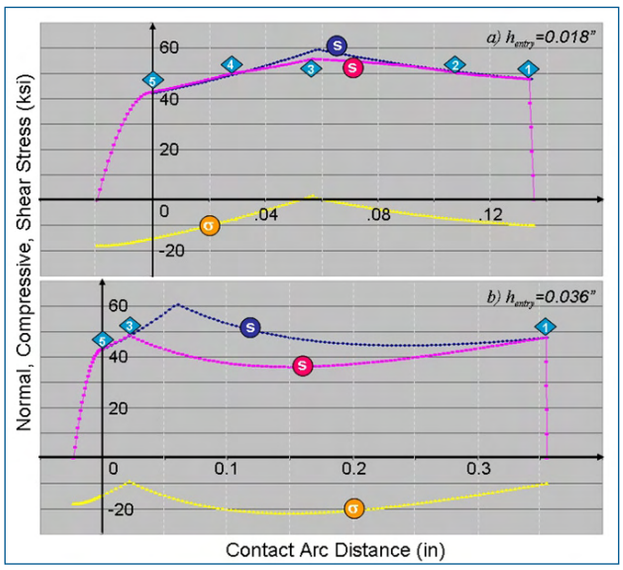

Fig. 3 - Influence of Entry Gage h_{entry}

Fig. 3 - Influenza dello spessore d'ingresso $h_{ingresso}$

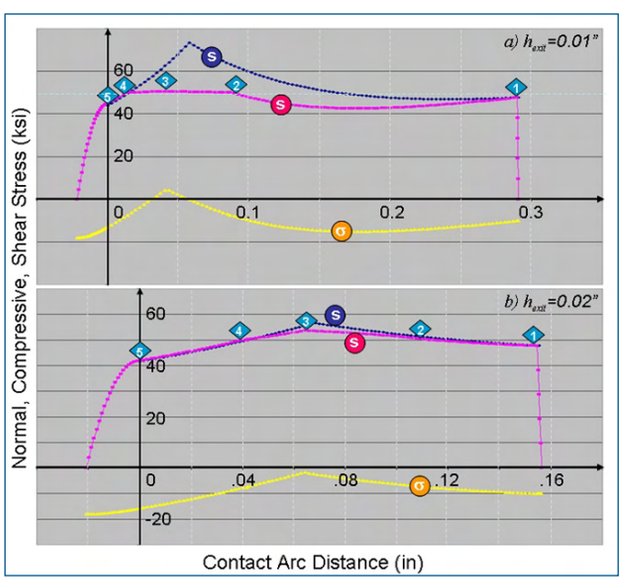

Fig. 4 - Influence of Exit Gage h_{exit}

Fig. 4 - Influenza dello spessore di uscita h_{uscita}

Influences of Exit Thicknesses

Figure 4 shows the influences due to the exit thickness. For the smaller exit gage of 0.01" (58.3% reduction), Figure 4a shows much larger roll bite, which is just slightly smaller than the case of entry gage of 0.036" (58.3% reduction). BAF shows a similar trend to the previous case – a friction hill is generated by the normal stress curves from both sides and the neutral point is located toward the exit side.

The results obtained from KEF have obvious differences. The trends of the normal and the compressive stress curves at the entry side are the same as the previous. As seen in Figure 4a, the normal stress from the entry side reaches the yield stress at the 2nd key node. In the loading stress-strain zone, KEF shows that the normal stress increment is very limited due to small strain increment. Two stress curves have significant differences – BAF stress is much larger than KEF stress. As to the exit side, two models have nearly the same normal stress curves in the small unyielding zone. After arriving at the yield point (the 4th key node), KEF limits the normal stress in the unloading stress-strain zone while BAF allows the increasing stress trend to satisfy the yield criterion. As with the previous case, BAF's neutral point is located at the right side of KEF's.
The thicker exit gage reduces the gage reduction (only 16.7%) and decreases the contact arc. The stress curves shown in Figure 4b looks like those curves shown in Figure 3a. The contact arc is slightly larger. The strip elements are subjected to tensile stresses in the roll bite. Two neutral points are almost at the same location. BAF's neutral point is slightly on the right side of KEF's neutral point. Although the entry bite distances x_1 are about twice difference, the exit bite distances are very close; *x=-0.0215*" for the thin exit gage of 0.01" and *x=-0.0208*" for the thicker exit gage of 0.02". The same phenomenon happens in the previous case that the thin entry gage of 0.018" is *x=-0.0197*" and the thick entry gage of 0.036" is *x=-0.0234*". It implies that rolling parameters do not have significant influences on the exit side bite angle.

Influences of Entry Tension Stress

Experiences show that strip tensions on both sides have large influences in rolling feasibility, the neutral point, the rolling force, and even the rolling power. For the ultra-thin gage rolling, the back tension is applied to control the target gage more effectively than the roll gap control, which shows the importance of the back tension.
As shown in Figure 5a, the material yields at the end of the elastic deformation zone if no entry tension is applied. Key nodes 1 and 2 happen to be the same. There is no yielding zone in the entry side. The material enters the loading stress-strain zone directly. The normal stress increases very quick due to the large strain increment. The compressive stress increases as well and the strip elements in the entry side are subjected to compressive stress only. The beginning node of the elastic recovery zone has a normal stress less than the yield stress. Two normal stress curves in the unyielding zone (between key nodes 4 and 5) are nearly the same. After passing the 4th key node, KEF shows that the normal stress increases rapidly to meet the normal stress curve from the entry side at the neutral point. The maximum stress is 96.4 ksi, which is about 1.93 times of the yield stress. Most carbon steel has the ultimate to yield stress ratio of less than 1.89. Stainless steel can go up to 2.51. Hence, from KEF viewpoint, this case should be "rolling impossible" for the carbon steel and "rolling feasible" for stainless steel. On the other hand, BAF does not consider the elastic deformation zone and the stress-strain curve. It starts from a higher entry normal stress point (57.75ksi) climbs up to the friction hill. The starting point at the exit side is located close to the 5th key node. Two normal stress curves generate a friction hill. This is a normal case to get the solution using BAF regardless of the material properties.

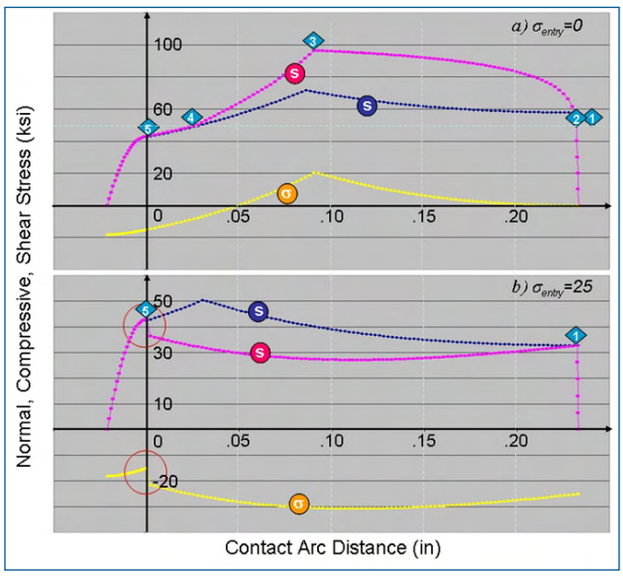

Figure 5: Influence of Entry Tension σ_{entry}

Figure 5: Influence of Entry Tension σ_{entry}

The general rule asserts that increasing the back tension push the neutral point toward the exit side. It also increases the dragging force to the strip. Larger entry tension may make rolling impossible. Figure 5b shows that the normal stress at the 1st key node is lower than the yield stress; hence, two models will start from the same 1st key node. As usual, KEF decreases and increases the normal stress following the yield criterion toward to the exit side while BAF increases the normal stress to form the friction hill. As to the exit side, the normal stress of the 5th key node is smaller than the yield stress. BAF has no problems to increase the normal stress and establish the friction hill after intercepting with the stress curve from the entry side. KEF must increase the normal and compressive stresses from the 5th key node to obtain the solution. However, since the stresses from the entry side at the 5th key node are smaller (see the red circle part shown in Figure 5b), there are no intercepts for both normal and compressive stress curves. Consequently, this case with a large back tension of 25 ksi is not legal from KEF's viewpoint, but it is legal from BAF's viewpoint.

Influences of Exit Tension Stress

Likewise, the exit tension should have influences on the roll bite behavior – increasing the exit tension should shift the neutral point toward the entry side. The larger exit tension can help the strip getting out of the roll bite. Since

the exit tension has a large contribution to the von Mises stress at the onset point of the elastic recovery zone, it determines the "state" of the onset point. For small exit tension, the material may reach the yield point, otherwise the material may yield by the Mises-Tresca yield criterion if the large exit tension is applied. Experience shows that the exit tension is not as effective as the entry tension, particularly, for the thin gage cases. However, it is a good on-line adjustment tool for the operator since it is not very sensitive to alter the rolling condition in a large scale.

Figure 6a shows the influences on the stress curves due to no exit tension. Two models will start from the same 1st key node following von Mises' yield criterion and von Karman's equation. BAF increases the normal stress rapidly while KEF increases the normal stress in a very slow pace. After reaching the 2nd key node, the material enters the stress-strain zone, which limits the normal stress increment even more and forms a small "bump" at the neighborhood of the neutral point. The compressive stress decreases slightly at the early part of the entry side, and then increases progressively until meeting the compressive curve from the exit side. The exit side has no tension, which drives the exit side normal stress high enough to hit the yield stress at the beginning of the elastic recovery zone. Key nodes 4 and 5 are identical. KEF forces the material to step into the unloading stress-strain zone to meet the stress curve from the entry side. The normal stress curve looks like a rectangular platform. BAF starts from a higher normal stress and generates a friction hill as usual. For the large exit tension case, the neutral points are shifted toward the entry side. The side shift distances are about the same for both models. The entry side behavior does not change since the entry tension remains the same. For the exit side, both models start from the same node, enter the unyielding zone, and have the nearly same normal stress curve in this zone. After the 4th key node, KEF follows the stress-strain curve while BAF allows the normal stress to increase so as to satisfy the yield criterion. The neutral point can be found easily in Figure 6b. The normal stress of KEF is smaller. The rolling force of KEF is slightly less than that of BAF.

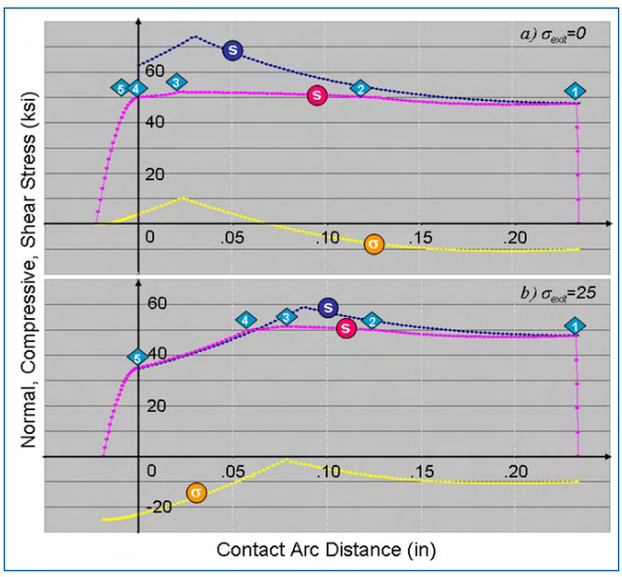

Fig. 6 - Influence of Exit Tension σ_{exit}

Fig. 6 - Influenza della tensione di uscita σ_{uscita}

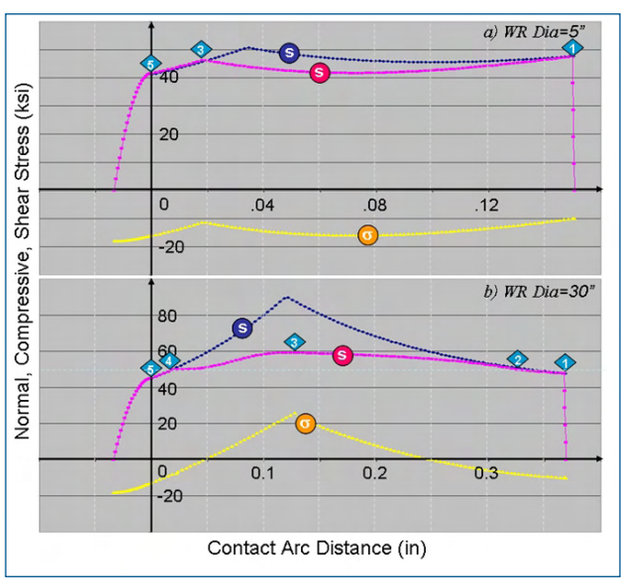

Fig. 7 - Influence of WR Diameter

Fig. 7 - Influenza del diametro WR

Influences of Work Roll Diameter

The smaller work roll has larger roll deflection and smaller indentation. It is suitable to perform thin gage rolling since the small indentation can prevent from the roll body contact. On the other hand, the smaller roll will deflect more and cause the roll edge to contact, which makes rolling not possible. For this typical cold rolling case, both models provide different solutions.

Figure 7a shows the stress components for the small work roll of 5". KEF does not have loading and unloading stress-strain zones. For both models, only yielding and unyielding zones in the plastic zone. BAF demonstrates a friction hill with "uphill" on both sides while KEF has a friction hill with "uphill" on the exit side and "down-and-up hill" on the entry side. The normal stress at the 5th key node is about 8% below the yield stress. The results of the unyielding zones are nearly the same. The entry side shows two normal stress curves split from the 1st key node. KEF's neutral point is located at the left side of BAF's neutral point. BAF's normal stress curve is greater in the entry side. The compressive stress remains negative in the roll bite; hence, the strip element is subjected to tensile stress in the entire roll bite. The rolling force is about the same for both models.

BAF shows a larger friction hill as shown in Figure 7b as the work roll diameter increases to 30" and the roll bite length becomes double. KEF has all five key nodes and

six characteristic zones. Again, the results of yielding and unyielding zones from both models are nearly the same. After the 2nd and 4th key nodes, BAF continues promoting the normal stress to form a large friction hill, while KEF enters the loading and unloading stress-strain zone with limited stress increment. The compressive stress increases from both sides much faster than the small work roll case. The locations of two neutral points are very close although they are the intercepts of two different stress curves - BAF uses the normal stress curves and KEF uses the compressive stress curves. KEF's rolling force is smaller in the case.

Influences of Yield Stress

As seen from Figure 8, the yield stress has a large influence on the normal stress distribution and the rolling force per unit width according to KEF. Figure 8a shows that the material does not yield at the end of the elastic zones. There are no loading and unloading stress-strain zones. The entry side normal stress curve goes downhill slightly to *x=0.167*, and then goes uphill until arriving at the neutral point. Two models have the same exit side normal stress curves and two friction hills.
When the yield stress becomes three (3) times lager, the material yields at the end points of the elastic zones. Key nodes 1 and 2 overlap and the material enter the loading stress-strain zone. The normal stress increases very fast to become more than 160 ksi (178% of the yield stress). As mentioned in Section 3.3, the normal stress should not surpass the ultimate stress to prevent from strip breakage in the roll bite. The ultimate stress of the rolled material should be checked to ensure rolling feasibility. If the rolling is feasible for certain materials, the large normal stress from the entry side creates a large "vertical drop" in the exit side. In the unloading stress-strain zone, the normal stress drops very quick, passes the inflection point, and arrives at key nodes 4 and 5 where the material yields at the onset point of the elastic recovery zone. KEF's normal stress curve is much larger than that BAF's although the neutral points of two models are very close.

Influences of Friction Coefficient

The friction coefficient is one of the largest influential parameters affecting rolling phenomenon. In general, it ranges from 0.03 (good lubrication) to 0.3 (dry rolling). Larger friction coefficient leads to larger shear stress which results in larger compressive stress that increases the normal stress and the shear stress. This consecutive and recursive stress increasing cycle drives the stress components to exceed its corresponding yield stress possibly. Frequently, the large friction coefficient causes the mill instability unless a small reduction is taken.
Figure 9a shows the stress curves with a small friction coefficient of 0.03. Both models have two zones – yielding and unyielding – in the plastic zone. KEF has the neutral point closer to the exit side. The strip element is always subjected to tensile stress. KEF's rolling force is slightly

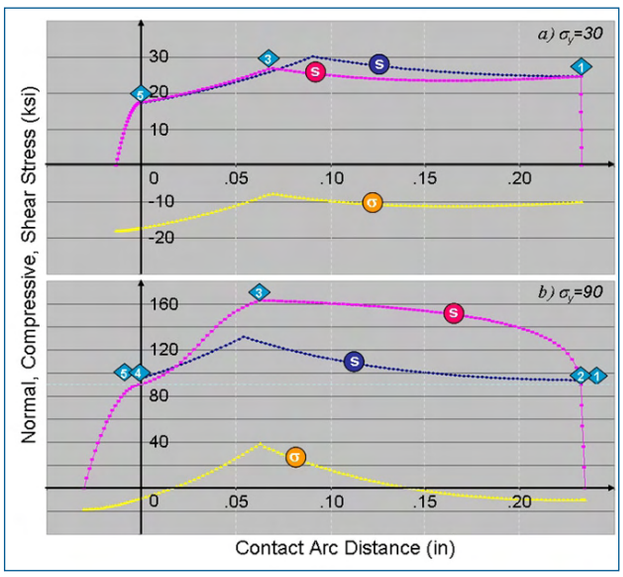

Fig. 8 - Influence of Yield Stress σ_y

Fig. 8 - Influenza del carico di snervamento σ_y

less than BAF's. These results are very typical by observing Figures 2b, 6a, 7a, and 8a. It implies that the neglected term $(s/K-1)d(hK)/d\phi$ in the governing equation, the neglected shear stress in the yield criterion, and the elastic foundation have a large effect in the entry side and have an insignificant effect in the exit side if the material does not yield at the 5th key node.
As to the dry rolling case, Figure 9b shows that BAF drives a normal stress to 820 ksi, which is 16.4 times of the yield stress and is definitely larger than the ultimate stress. Rolling should not be possible if the ultimate stress is considered. On the other hand, KEF shows that the material yields at the beginning of the elastic recovery zone (key nodes 4 and 5 overlap). There is a small yielding zone in the entry side after the elastic deformation zone (key nodes 1 and 2 separated). Due to the large friction coefficient, the compressive stress increases very fast and exceeds the yield stress at *x=0.0187*" and *x=0.187*". There are two red circles at the intercept points of the normal and compressive stress curves. If von Karman's equation holds in the x ranging between these two red circles, then the compressive stress curves violate the material properties (exceeding the yield stress). If the model limits the compressive stress to the yield stress, then von Karman's equation will no longer be true. Hence, the solution does not exist as soon as the compressive stress curve surpasses the normal stress curve. Consequently, KEF will declare "roll impossible" for high friction coefficient cases while BAF may still produce the solution.

CONCLUSION AND DISCUSSION

This article has described a method to solve von Karman's equation on the elastic foundation. von Karman's equation was derived from the equilibrium condition of an in-

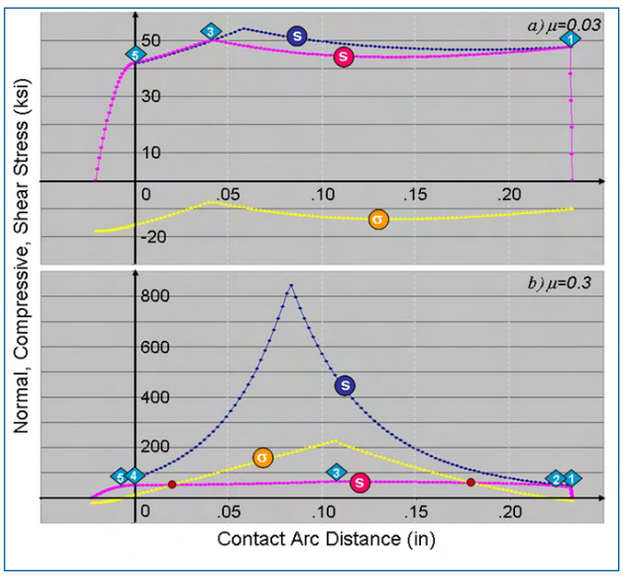

***Fig. 9 - Influence of Friction Coefficient* μ**

Fig. 9 - Influenza del coefficiente di attrito μ

finitesimal element in the roll bite. The equation should be applicable to all rolling cases regardless of mill types and operating conditions. Without doubt, the roll indentation should be considered to better reflect the real-world rolling condition. Experiences show that separation of the governing equation and the roll indentation equation will cause numerical instability since the calculated roll contour of the current step will recursively reduces the entry bite angle and increases the exit bite angle in the next step. The concept of applying the elastic foundation to von Karman's equation can simplify the theoretical derivation and preserve the numerical stability to obtain the solution. The proposed model asserts that the material obey Hooke's law in the elastic zones, follow von Mises' yield criterion in the plastic yielding and unyielding zones, and trace the material stress-strain curve in the plastic loading and unloading zones. The boundary conditions from two ends of the roll bite should be propagated inward to the core portion of the roll bite. The end result of the previous zone specifies the boundary condition for the next zone. The join point between two zones, which is referred to "key node" in this article, satisfies the specific characteristics of two adjacent zones. As a result, the roll bite may include five key nodes and six characteristic zones. The entry elastic deformation zone and the exit elastic recovery zone always exist for all rolling cases. The existence of other four plastic zones completely depends on the imposed rolling parameters. The calculation results show that the compressive stress curve looks like the "friction hill" as described in the conventional methods. However, this is a modified friction hill with an uphill in the exit side, but an uphill or a down-and-up hill in the entry side. The neutral point can be easily found from the compressive stress curve as the tip of the "compressive friction hill". The normal stress curve has various shapes depending on the possession of characteristic zones. In case of no stress-strain zones, the curve looks more like a modified friction hill since the survived yielding and unyielding zones are also applied in the conventional investigations. If the stress-strain zones do exist, the curve looks more like a "platform" or a "van". Frequently, the neighborhood of the neutral point becomes very flat, which makes difficulties to locate the neutral point without helps from the compressive stress curves.

The case study focuses on the result comparison between KEF (von Karman's Equation on the Elastic Foundation) model and BAF (Bland-and-Ford) model. As shown in some study cases, KEF's solutions in the unyielding zone are nearly the same as BAF while the solutions in the yielding zone have trivial differences. This is due to that BAF neglects one term in the governing equation and the shear stress term in von Mises' criterion. Besides of these differences, two models have a very good agreement in all study cases. BAF's rolling feasibility relies on whether or not the friction hill can be found. However, KEF emphasizes on whether or not the solution can meet the physical meanings of material properties. KEF's criteria of rolling feasibility are (a) the normal stress cannot exceed the ultimate stress of the material, (b) the compressive stress cannot be greater than the yield stress considering the local work hardening, (c) the compressive stress curve cannot intercept with the normal stress curve, (d) the normal stress at the exit plastic zones cannot decrease as the bite angle increases. These criteria have been reiterated in the study cases.

There are many trials and modifications when developing this new method. Based on the current test cases and comparison results, the model can provide reasonable results for various rolling conditions. This article focuses on the cold rolling cases only. As mentioned before, the model should be applicable to any rolling condition. Hence, the future research will continue to verify the model on various rolling types – from the thickest gage of the plate mill to the thinnest gage of the foil mill, from the lightest reduction of the skin pass mill to the heaviest reduction of the bonding mill, and from the smallest roll of the cluster mill to the largest roll of the two high vertical stack mill. Other rolling parameters will be tested and evaluated as well. The present satisfactory results definitely encourage the development of the future research outlook.

ACKNOWLEDGEMENT

The author likes to thank Tenova's management team for their R&D support and approval for this paper to be presented and published.

REFERENCES

1. T. Von Karman, "Beitrag zur theorie des walzvorganges", Zeitschrift fur Angewandte, Mathematik und Mechanik 5, 1925, 139-141
2. R. B. Sims, "Calculation of roll force and torque in hot rolling mills", Proceedings of the Institute of Mechani-

cal Engineers, London 169, 1954, 191

3. D. R. Bland, H. Ford, “The calculation of roll force and torque in cold strip rolling with tensions”, Proceedings of the Institute of Mechanical Engineers, London 159, 1948, 144-163
4. W. L. Roberts, “Cold Rolling of Steel”, Marcel Dekker, Inc. New York and Basel, 1978, pp 478
5. N. A. Fleck, K. L. Johnson, “Towards a new theory of cold rolling thin foil”, Int., J. Mech. Sci, 1987, Vol. 29, No. 7, 507-524
6. N. A. Fleck, et. al., “Cold rolling of foil”, Proc. Instn. Mech. Engrs, vol. 206, pp 119-131, IMechE 1992
7. Y. Liu and W. H. Lee, “Mathematical Model for the Thin Strip Cold Rolling and Temper Rolling Process with the Influence Function Method”, ISIJ International, vol. 45 (2005), No. 8, pp 1173-1178.
8. Roark, R. J. & Young W. C., “Formulas for Stress and Strain”, McGraw-Hill Inc., 1975, 513-530
9. R. Guo, “A Semn-Analytical Solution of von Karman Rolling Equation with Infinitely Rigid Rolls – Part I”, Iron and Steel Technology AIST, Nov. 2013, vol. 10, No.11, pp 65-80
10. R. Guo, “A Semn-Analytical Solution of von Karman Rolling Equation with Roll Indentation – Part II”, Iron and Steel Technology AIST, Feb. 2014, vol. 11, No.2, pp 79-95

Investigazione sul comportamento dell’area di contatto tra i rulli di lavoro nella laminazione a freddo usando soluzioni semianalitiche delle equazioni di von Karman

Parole chiave: Deformazioni plastiche - Laminazione

Questo articolo propone una soluzione semi-analitica dell’equazione di laminazione di von Karman basandosi sulla teoria della fondazione elastica. La deformazione dei rulli è considerata come la compressione della fondazione elastica di una molla. Un contatto d’arco non circolare si ottiene naturalmente come una parte della soluzione dell’equazione di governo. Due zone elastiche e quattro zone plastiche sono considerate. La legge di Hooke è applicata nelle zone elastiche , il criterio di snervamento di von Mises viene utilizzato nella zona di snervamento e non snervamento plastico e le curve sforzo-deformazione dei materiale sono impiegate nell zone di carico e non carico plastico. La soluzione in ogni zona viene derivata separatamente e un programma di calcolo viene progettato conseguentemente. Il tempo di elaborazione è molto breve e il nucleo di memoria richiesto è molto piccolo. I risultati mostrano che le curve di sforzo a compressione formano una “ collina di attrito” mentre la forma della curva di sforzo normale dipende dai parametri di laminazione. Un tipico caso di laminazione a freddo è selezionato come caso basico di studio. I risultati di questo proposta di modello e i risultati relativi al famoso modello di Bland e- Ford sono mostrati per essere paragonati tra di loro . Parametri fondamentali inclusi in questo paragone sono lo spessore del nastro in ingresso, lo spessore in uscita, la tensione del nastro in ingresso, la tensione in uscita, il diametro del cilindro di lavoro, lo snervamento del materiale e il coefficiente di attrito. La fattibilità sulla laminazione derivata da questo modello proposto non è solo data dall’esistenza della convergenza delle soluzione ma anche dalla possibilità o meno che la soluzione segua le proprietà del materiale laminato.